

Exact decoherence and entanglement dynamics in homogeneous two-qubit XXZ central spin models

Zejiang Li,¹ Pei Yang,¹ Wen-Long You,^{2,3} and Ning Wu^{1,*}

¹*Center for Quantum Technology Research, School of Physics,
Beijing Institute of Technology, Beijing 100081, China*

²*College of Science, Nanjing University of Aeronautics and Astronautics, Nanjing 211106, China*
³*School of Physical Science and Technology, Soochow University, Suzhou, Jiangsu 215006, China*

We obtain exact reduced dynamics of two interacting qubits homogeneously coupled to spin baths via the XXZ -type hyperfine interaction, with the baths prepared in the spin coherent state. By working in the interaction picture with respect to the non-spin-flipping part of the Hamiltonian, evaluating the time evolution of the whole system is converted to solving a sequence of equations of motion within each magnetization sector. We first study the single-qubit decoherence for which closed-form solutions exist. The observed collapse and revival behaviors of the single-qubit Rabi oscillation are quantitatively explained by investigating the detailed structure of the time-evolved state. We then study the disentanglement and coherence dynamics of two initially entangled noninteracting qubits when the two qubits interact with individual baths or with a common bath. We find that for individual baths the coherent dynamics is positively correlated to the single-qubit purity dynamics, and entanglement sudden disappearance and subsequent revivals are observed in both cases due to the non-Makovian nature of the spin baths. The entanglement creation of two initially separable qubits coupled to a common bath is finally studied. We observe collapse and revival behaviors in the entanglement dynamics, thus providing a possible scheme to realize steady and finite two-qubit entanglement over relatively long periods of time.

I. INTRODUCTION

The reduced dynamics of simple quantum systems under the influence of structured spin environments [1] has long been a widely studied topic because of its high relevance to quantum decoherence [2–16] and quantum information sciences [17–24], excitation energy transfer [25–27], mathematical physics [28–39], and also on. Among these, the so-called spin-star network consisting of a preferred central spin coupled to a spin bath without intra-bath interactions has attracted much attention due to its exact solvability under certain conditions [5, 10, 12, 26–39]. Specifically, when the coupling between the central spin and the spin bath is homogeneous, the spin bath can be treated as a “big spin” composed of the surrounding bath spins [12, 13, 35, 37]. Although the such obtained homogeneous model looks simple at first sight, it still contains rich physics and possesses elegant mathematical structures. For example, the exact spectrum of a homogeneous isotropic (or XXX) central spin model with arbitrary central spin size is determined based on the algebraic properties and integrability of the model [35]. The central spin dynamics in a spin-1/2 homogeneous XXZ central spin model is obtained analytically using a recurrence method based on an expansion of the time-evolution operator [37]. It is shown recently that the homogeneous anisotropic (or XX) central spin model with spin-1/2 central spin and arbitrary bath-spin sizes is solvable via the Bethe ansatz [38, 39].

In this work, we consider a generalization of the single-

qubit homogenous XXZ central spin model to the case of two interacting central spins. Based on the big-spin description of the spin bath, we are interested in the decoherence and entanglement dynamics of the two-qubit system under the influence of the spin baths. The reduced dynamics of a pair of qubits coupled to individual or common bosonic baths has been widely studied in the context of quantum optics, mainly based on theoretical tools such as Markovian or non-Markovian quantum master equations [40–57]. In special, Yu and Eberly [42] found using Markovian quantum master equations that two initially entangled two-level atoms coupled to their own photonic baths can disappear in a finite time due the spontaneous emission. Bellomo *et al.* [45] showed in the same setup that a revival of the disappeared entanglement happens if non-Markovian quantum master equations are adopted. In general, the coupling of central spins to a spin environment can lead to non-Markovian behaviors [58–60], which renders the application of usual Markovian quantum master equations difficult for such systems. Previous studies on the dynamics of two-qubit central spin systems usually assume thermal states at finite/infinite temperatures for the bath initial state [5, 15, 20, 61]. Due to the close analogy between the qubit-big spin model and the Jaynes-Cummings model in quantum optics [12, 37], it is an interesting option to prepare the spin bath in the so-called spin coherent state, which is an analog of a coherent state for an optical field. It has been shown in Refs. [12, 13, 37] that the collapse and revival phenomena originally observed in the Jaynes-Cummings model [62] also occur in the qubit-big spin model.

By focusing on the two-qubit-big spin system with magnetization-conserving XXZ -type system-bath coupling, we consider real-time dynamics of the system in

*Electronic address: wun1985@gmail.com

two situations: (a) Each of the two qubits interacts with its own spin bath; (b) The two qubits interact with a common spin bath. We choose *spin coherent state* as the bath initial state and show that in both cases the exact reduced dynamics of the two-qubit system can be conveniently obtained by using the interaction picture Hamiltonian with respect to the *non-spin-flipping* part of the model. In case (a) with individual baths, the two-qubit dynamics is directly determined by the single-qubit dynamics [45]. We show that the exact single-qubit dynamics presented in Ref. [37] can be alternatively derived in the interaction picture through analytically solving the coupled equations of motion in each magnetization sector. Moreover, we show that the collapse and revival behaviors of the single-qubit Rabi oscillations observed in Refs. [12, 13, 37] can be *quantitatively* explained via an analogy of the structure of the time-evolved state to that of the Jaynes-Cummings model [62]. In case (b) with a common bath, we are able to obtain the time-evolution state of the whole system, with the amplitudes satisfying a sequence of systems of coupled equations in each four-dimensional sector with a fixed magnetization.

With the help of the analytical solution and numerical simulations of the equations of motion, we calculate time evolution of the concurrence [63] and relative entropy of coherence [64] for the two-qubit system. In the case of individual baths, we focus on the disentanglement dynamics of two initially entangled qubits without inter-qubit interaction. We find that entanglement sudden disappearance and later revivals happen due to the non-Markovian nature of the spin baths. We also find that the two-qubit coherence dynamics behaves similarly to the single-qubit purity dynamics in the single-qubit problem, indicating that the two quantities are positively correlated. When the two qubits interact with a common bath, we observe bath-mediated entanglement and coherence generation. In special, for bath initial states with certain polarizations, we find that collapse and revival phenomena can occur in the entanglement and coherence dynamics, which provides a possible scheme to dynamically generate long-lasting steady entanglement or coherence in the collapse regime.

The rest of the paper is organized as follows. In Sec. II we introduce our model and derive the interaction picture Hamiltonian for later use. In Sec. II the single-qubit problem is revisited and carefully studied. In Sec. IV we study the entanglement and coherence dynamics of the two-qubit system coupled to individual baths or to a common bath. Conclusions are drawn in Sec. V.

II. MODEL AND INTERACTION PICTURE HAMILTONIAN

We consider a composite system consisting of two qubits coupled to a spin bath made up of N noninteracting two-level systems [see Fig. 1(a)], which is described

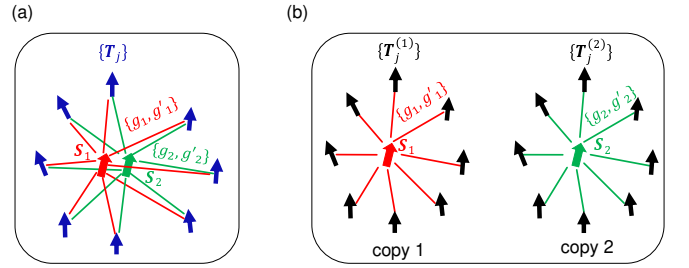


FIG. 1: (a) Two (interacting) central spins \vec{S}_1 and \vec{S}_2 interact with a common spin bath via the homogeneous XXZ -type coupling [see Eq.(1)]. (b) Two noninteracting central spins interact with their own spin baths [see Eq. (35)].

by the Hamiltonian

$$H = H_S + H_{SB}. \quad (1)$$

Here, H_S is the Hamiltonian for the two qubits that interact with each other via the XXZ -type coupling:

$$\begin{aligned} H_S &= H_{S,0} + H_{S,1}, \\ H_{S,0} &= \omega_1 S_1^z + \omega_2 S_2^z + 2J' S_1^z S_2^z, \\ H_{S,1} &= 2J(S_1^x S_2^x + S_1^y S_2^y). \end{aligned} \quad (2)$$

The system-bath coupling is also assumed to be of XXZ -type, and is described by

$$\begin{aligned} H_{SB} &= H_{SB,0} + H_{SB,1}, \\ H_{SB,0} &= 2 \sum_{i=1,2} \sum_{j=1}^N g'_i S_i^z T_j^z, \\ H_{SB,1} &= 2 \sum_{i=1,2} \sum_{j=1}^N g_i (S_i^x T_j^x + S_i^y T_j^y). \end{aligned} \quad (3)$$

In the above equations, S_i^α and T_j^α ($\alpha = x, y, z$) are the spin-1/2 operators of the i th ($i = 1, 2$) qubit and the j th ($j = 1, 2, \dots, N$) bath spin, respectively, J and J' are the qubit-qubit interaction strengths, and g_i and g'_i measure the system-bath coupling strength between the i th qubit and any of the bath spins. Note that each qubit interacts uniformly with the spin bath.

Since we have assumed that the spin bath has no intra-bath coupling, it is convenient to introduce the collective angular momentum operator for the spin bath,

$$L_\alpha = \sum_{j=1}^N T_j^\alpha, \quad \alpha = x, y, z. \quad (4)$$

It is easy to verify that the total magnetization of the whole system, $M = S_1^z + S_2^z + L_z$, is conserved. Another

obvious conserved quantity is the total angular momentum of the spin bath, $\vec{L}^2 = \sum_{\alpha} L_{\alpha}^2$. So if we start with an initial state with fixed l , where $l(l+1)$ denote the eigenvalue of \vec{L}^2 , then the evolved state will always belong to this l -subspace. We will use the simultaneous eigenstates of \vec{L}^2 and L_z , $\{|l, m\rangle\}$, as the basis states in the l -subspace of the spin bath. Note that \vec{L}^2 is no longer conserved if either intrabath coupling or inhomogeneity in the system-bath coupling g_j is introduced [13].

Throughout this paper we will adopt the spin coherent state $|\hat{\Omega}\rangle$ as the initial state for the spin bath [12, 13, 37]. A spin coherent state for the N bath spins exists in the $l = N/2$ subspace of the bath and is parameterized by the unit vector $\hat{\Omega} = (\sin \theta \cos \phi, \sin \theta \sin \phi, \cos \theta)$. Starting with the fully polarized state $|\frac{N}{2}, \frac{N}{2}\rangle = \otimes_{j=1}^N |+\rangle_j$, where $|+\rangle_j$ is the spin-up state of the j th bath spin, $|\hat{\Omega}\rangle$ can be obtained by first rotating about the y -axis by an angle θ , followed by a rotation about the z -axis by an angle ϕ . The spin coherent state $|\hat{\Omega}\rangle$ can be written as [65]

$$\begin{aligned} |\hat{\Omega}\rangle &= e^{-iL_z\phi} e^{-iL_y\theta} \left| \frac{N}{2}, \frac{N}{2} \right\rangle \\ &= \sum_{n=0}^N Q_n \left| \frac{N}{2}, n - \frac{N}{2} \right\rangle, \end{aligned} \quad (5)$$

with

$$Q_n = \frac{z^n}{(1+|z|^2)^{N/2}} \sqrt{C_N^n}, \quad (6)$$

where $z \equiv \cot \frac{\theta}{2} e^{-i\phi}$ and $C_N^n = \frac{N!}{n!(N-n)!}$ is the binomial coefficient. For the sake of clarity, we present in Appendix A the derivation of the second line of Eq. (5). Here, $|\frac{N}{2}, n - \frac{N}{2}\rangle$ ($n = 0, 1, \dots, N$) is the fully symmetric Dicke state which is the simultaneous eigenstate of \vec{L}^2 and L_z with eigenvalues $\frac{N}{2}(\frac{N}{2}+1)$ and $n - \frac{N}{2}$.

As will be shown later, to study the real-time dynamics of the system, it turns out to be convenient to work in the interaction picture with respect to the non-spin-flipping part of H , i.e., $H_0 = H_{S,0} + H_{SB,0}$, so that all terms in H_0 commute with each other. A straightforward calculation gives the following interaction picture Hamiltonian for $H_1 = H_{S,1} + H_{SB,1}$,

$$\begin{aligned} H_I(t) &= e^{iH_0 t} H_1 e^{-iH_0 t} \\ &= J[e^{i2g'_{12}L_z t} e^{i\omega_{12}t} S_1^+ e^{-i2J'(S_1^z - S_2^z)t} S_2^- + \text{H.c.}] \\ &+ \left(\sum_k g_k S_k^- e^{-i\omega_k t - i2(J' S_k^z + g'_k L_z)t} \right) e^{i \sum_k 2g'_k S_k^z t} L_+ \\ &+ \text{H.c.}, \end{aligned} \quad (7)$$

where $S_k^{\pm} = S_k^x \pm iS_k^y$ ($k = 1, 2$), $L_{\pm} = L_x \pm iL_y$, $g'_{12} \equiv g'_1 - g'_2$, $\omega_{12} \equiv \omega_1 - \omega_2$, and $\tilde{1} = 2$, $\tilde{2} = 1$. The time-dependent interaction picture Hamiltonian $H_I(t)$ can be viewed as an extended two-qubit XX central spin model, where the effect of the Ising part of the XXZ -interaction in H has been absorbed into the spin lowering/raising operators.

III. REDUCED DYNAMICS OF THE SINGLE QUBIT

Before studying the two-qubit dynamics, let us first investigate the reduced dynamics of a single qubit coupled uniformly to the spin bath. We will use the Hamiltonian $H_I(t)$ in the interaction picture to derive the equations of motion for the amplitudes appearing in a general evolved state and solve them analytically. Based on the analytical solution, we provide a qualitative explanation of the observed collapse and revival phenomena [12, 13, 37].

A. Analytical form of the reduced density matrix

The interaction picture Hamiltonian for a single qubit, say qubit 1, can be obtained by setting $J = J' = \omega_2 = g_2 = g'_2 = 0$ in $H_I(t)$ given by Eq. (7),

$$H_I^{(1)}(t) = g_1 e^{-i\omega_1 t} S_1^- e^{-i2g'_1 L_z t} e^{i2g'_1 S_1^z t} L_+ + \text{H.c.} \quad (8)$$

We denote $|\uparrow\rangle$ ($|\downarrow\rangle$) as the up- (down-) state of the qubit and choose the initial state to be a product state,

$$|\psi_0^{(1)}\rangle = |\varphi^{(1)}\rangle \otimes |\hat{\Omega}\rangle, \quad (9)$$

where

$$|\varphi^{(1)}\rangle = \sum_{s=\uparrow,\downarrow} f_s |s\rangle, \quad (10)$$

is a generic state for qubit 1 with $\sum_{s=\uparrow,\downarrow} |f_s|^2 = 1$. To simplify the notations, we denote $|m\rangle$ as the bath state $|\frac{N}{2}, m\rangle$ and let $L \equiv N/2$. There are totally $D_{\text{tot}}^{(1)} = 2(N+1)$ basis states of the form $|s\rangle |n-L\rangle$ ($s = \uparrow, \downarrow$ and $n = 0, \dots, N$), which are arranged in order as

$$\begin{aligned} &|\downarrow\rangle | -L \rangle, \\ &|\uparrow\rangle | -L \rangle, |\downarrow\rangle | -L+1 \rangle, \\ &|\uparrow\rangle | -L+1 \rangle, |\downarrow\rangle | -L+2 \rangle, \\ &\vdots \\ &|\uparrow\rangle |L-1 \rangle, |\downarrow\rangle |L \rangle \\ &|\uparrow\rangle |L \rangle. \end{aligned}$$

We write the general time-evolved state in the interaction picture as

$$|\psi_I^{(1)}(t)\rangle = \sum_{s=\uparrow,\downarrow} \sum_{n=0}^N F_s^{(n)}(t) |s\rangle |n-L\rangle, \quad (11)$$

with initial conditions

$$F_s^{(n)}(0) = f_s Q_n, \quad (12)$$

where $\{F_s^{(n)}(t)\}$ are $D_{\text{tot}}^{(1)}$ time-dependent amplitudes determined by the time-dependent Schrödinger equation $i\partial_t |\psi_I^{(1)}(t)\rangle = H_I(t) |\psi_I^{(1)}(t)\rangle$. It is easy to see that

$$F_{\downarrow}^{(0)}(t) = f_{\downarrow} Q_0, \quad F_{\uparrow}^{(N)}(t) = f_{\uparrow} Q_N \quad (13)$$

are constants since $H^{(1)}(t)|\downarrow\rangle|L\rangle = H^{(1)}(t)|\uparrow\rangle|L\rangle = 0$. Due to the conservation of $S_1^z + L_z$, the time evolution takes place separately within each row, yielding the following equations of motion for the two components $F_{\downarrow}^{(n)}(t)$ and $F_{\uparrow}^{(n-1)}(t)$ (see Appendix B):

$$\begin{aligned} i\dot{F}_{\uparrow}^{(n-1)}(t) &= F_{\downarrow}^{(n)}(t)g_1x_{n-L-1}e^{-ig_1't}e^{i2g_1'(n-L)t}e^{i\omega_1t}, \\ i\dot{F}_{\downarrow}^{(n)}(t) &= F_{\uparrow}^{(n-1)}(t)g_1x_{n-L-1}e^{-i\omega_1t}e^{-i2g_1'(n-L)t}e^{ig_1't}. \end{aligned} \quad (14)$$

where $n = 1, 2, \dots, N$ and

$$x_m \equiv \sqrt{(L-m)(L+m+1)}. \quad (15)$$

It is shown in Appendix C that the analytical solutions of Eqs. (13) and (14) with initial conditions given by Eq. (12) can be written as

$$\begin{aligned} F_{\uparrow}^{(n)}(t) &= e^{\frac{i}{2}b_{n+1}t}(f_{\uparrow}Q_nW_{n+1} + f_{\downarrow}Q_{n+1}V_{n+1}), \\ F_{\downarrow}^{(n)}(t) &= e^{-\frac{i}{2}b_n t}(f_{\downarrow}Q_nW_n^* + f_{\uparrow}Q_{n-1}V_n), \end{aligned} \quad (16)$$

for $n = 0, 1, \dots, N$. Here,

$$W_n \equiv \begin{cases} \cos \frac{A_n t}{2} - i \frac{b_n}{A_n} \sin \frac{A_n t}{2}, & n = 1, 2, \dots, N \\ e^{-i \frac{b_n t}{2}}, & n = 0 \text{ or } N+1 \end{cases} \quad (17)$$

and

$$V_n \equiv \begin{cases} -i \frac{2a_n}{A_n} \sin \frac{A_n t}{2}, & n = 1, 2, \dots, N \\ 0, & n = 0 \text{ or } N+1 \end{cases} \quad (18)$$

with

$$\begin{aligned} a_n &\equiv g_1x_{n-L-1} = a_{N+1-n}, \\ b_n &\equiv \omega_1 + g_1'[2(n-L) - 1], \\ A_n &\equiv \sqrt{b_n^2 + 4a_n^2}. \end{aligned} \quad (19)$$

Note that $a_0 = a_{N+1} = 0$ and $|W_n|^2 + |V_n|^2 = 1$.

The Schrödinger picture wave function reads

$$\begin{aligned} |\psi^{(1)}(t)\rangle &= e^{-i(\omega_1 S_1^z + 2g_1' S_1^z L_z)t} |\psi_I^{(1)}(t)\rangle \\ &= \sum_{s=\uparrow,\downarrow} \sum_{n=0}^N \tilde{F}_s^{(n)}(t) |s\rangle |n-L\rangle, \end{aligned} \quad (20)$$

where

$$\begin{aligned} \tilde{F}_{\uparrow}^{(n)}(t) &\equiv e^{-i\frac{1}{2}(b_n+g_1')t} F_{\uparrow}^{(n)}(t), \\ \tilde{F}_{\downarrow}^{(n)}(t) &\equiv e^{i\frac{1}{2}(b_n+g_1')t} F_{\downarrow}^{(n)}(t). \end{aligned} \quad (21)$$

The reduced density matrix of the qubit \vec{S}_1 can be obtained by tracing out the bath degrees of freedom

$$\begin{aligned} \rho^{(1)}(t) &= \text{Tr}_B(|\psi^{(1)}(t)\rangle\langle\psi^{(1)}(t)|) \\ &= \sum_{ss'} \left[\sum_n \tilde{F}_s^{(n)}(t) \tilde{F}_{s'}^{(n)*}(t) \right] |s\rangle\langle s'|, \end{aligned} \quad (22)$$

with the initial density matrix given by

$$\rho^{(1)}(0) = \sum_{ss'} f_s f_{s'}^* |s\rangle\langle s'|. \quad (23)$$

In the basis $\{|\uparrow\rangle, |\downarrow\rangle\}$, the time-evolved density matrix $\rho^{(1)}(t)$ is connected with $\rho^{(1)}(0)$ via the relations

$$\rho_{ab}^{(1)}(t) = \sum_{cd} Y_{abcd}(t) \rho_{cd}^{(1)}(0), \quad (24)$$

where $\rho_{ab}^{(1)}(t) = \langle a|\rho^{(1)}(t)|b\rangle$ ($|a\rangle, |b\rangle = |\uparrow\rangle$ or $|\downarrow\rangle$). Using Eqs. (16) and (21), we can directly obtain the explicit forms of the coefficients $\{Y_{abcd}(t)\}$, which are listed in Appendix D. Equation (24) provides the complete information for the reduced dynamics of qubit 1. Below we will use these results to study the dynamics of various single-qubit observables.

B. Polarization and purity dynamics

We suppose that the central spin is initially in its up-state, i.e., $f_{\uparrow} = 1$ and $f_{\downarrow} = 0$, then the polarization $\langle S_1^z(t) \rangle$ can be expressed as

$$\begin{aligned} \langle S_1^z(t) \rangle &= \frac{1}{2} [\rho_{\uparrow\uparrow}^{(1)}(t) - \rho_{\downarrow\downarrow}^{(1)}(t)] \\ &= \frac{1}{2} \sum_{n=0}^N |Q_n|^2 \frac{b_{n+1}^2 + 4a_{n+1}^2 \cos A_{n+1}t}{A_{n+1}^2}, \end{aligned} \quad (25)$$

which is in consistent with the result in Ref. [37].

The off-diagonal element of $\rho^{(1)}(t)$ characterizes the coherence of the qubit and is given by $\langle S_1^+(t) \rangle = \rho_{\downarrow\uparrow}^{(1)}(t)$, yielding

$$\begin{aligned} \langle S_1^x(t) \rangle &= \sum_{n=1}^N \frac{Q_n Q_{n-1} a_n b_{n+1}}{A_n A_{n+1}} \\ &\quad \left[\cos \frac{(A_n - A_{n+1})t}{2} - \cos \frac{(A_n + A_{n+1})t}{2} \right], \end{aligned} \quad (26)$$

and

$$\begin{aligned} \langle S_1^y(t) \rangle &= - \sum_{n=1}^N \frac{Q_n Q_{n-1} a_n}{A_n} \\ &\quad \left[\sin \frac{(A_n + A_{n+1})t}{2} + \sin \frac{(A_n - A_{n+1})t}{2} \right]. \end{aligned} \quad (27)$$

We also monitor the purity dynamics defined by

$$P(t) = \frac{1}{2} + 2 \sum_{i=x,y,z} \langle S_1^i(t) \rangle^2. \quad (28)$$

Below we will focus on two limiting cases, i.e., the fully anisotropic (XX -type coupling) and fully isotropic (XXX -type coupling) limit.

1. XX -type coupling: $g'_1 = 0$

First, we would like to mention that it is shown recently that the homogeneous XX central spin model is exactly solvable via the Bethe ansatz for $s_1 = 1/2$ and arbitrary $\{t_i\}$ [38] (t_i is the quantum number of the i th bath spin \vec{T}_i). The situation studied here amounts to the special case of $t_i = 1/2$, $\forall i$. Note that collapse and revival phenomena in such a model has been numerically revealed in Refs. [12, 13]. Here, we will provide a quantitative explanation of the observed collapse-revival phenomena.

We plot in Fig. 2 the dynamics of the three components $\langle S_1^\alpha(t) \rangle$ and the purity $P(t)$ starting from the upper state $|\uparrow\rangle$ of qubit 1 for four different values of θ ranging from $\theta = 0$ to $\theta = \pi/2$. It can be seen that for $\theta = \pi/10$ all quantities oscillate randomly and no features are developed as time evolves [Fig. 2(a)]. In the other extreme case with $\theta = \pi/2$, the purity $P(t)$ decreases gradually with slight oscillations and approaches a completely mixed state with $P = 1/2$ in the long-time limit [Fig. 2(d)]. In contrast, for $3\pi/10$, we first observe an abrupt collapse of the qubit state at a short-time scale, which is followed, to a good approximation, by a revival of some pure state with a high purity at $g_1 t \approx 2.1$. The approximate recreation of the state vector is accompanied by a collapse in $\langle S_1^z(t) \rangle$ and by nearly vanishing $\langle S_1^x(t) \rangle$, indicating that the reached qubit state is approximately the state pointing along the $-y$ direction.

The revival of the qubit state and collapse of the $\langle S_1^z(t) \rangle$ profile found in the present model with $g'_1 = 0$ are very similar to the phenomenon observed in the Jaynes-Cummings model [62] and the relationship between the two models was discussed in Refs. [12, 37]. To understand the above observations in the context of a spin bath, we note from Eqs. (16), (17), (18), and (20) that the time-evolved state $|\psi^{(1)}(t)\rangle$ depends on both the coefficients $\{Q_n\}$ characterizing the bath initial condition and the Rabi frequencies $\{A_n\}$. In Fig. 3(a) we plot $|Q_n|$ for several values of θ and find that for each one there is some $n = n_{\max}$ around which $|Q_n|$ is significantly different from zero. Suppose at some time t_r a revival of the qubit pure state is approximately achieved, then the state $|\psi^{(1)}(t_r)\rangle$ will have the form

$$|\psi^{(1)}(t_r)\rangle \approx \sum_{n \approx n_{\max}} \left[\sum_{s=\uparrow,\downarrow} \tilde{F}_s^{(n)}(t_r) |s\rangle \right] |n-L\rangle, \quad (29)$$

where the ratio between $\tilde{F}_\uparrow^{(n)}(t_r)$ and $\tilde{F}_\downarrow^{(n)}(t_r)$,

$$\begin{aligned} \frac{\tilde{F}_\uparrow^{(n)}(t_r)}{\tilde{F}_\downarrow^{(n)}(t_r)} &= \frac{Q_n W_{n+1}(t_r)}{Q_{n-1} V_n(t_r)} \\ &= \frac{Q_n}{Q_{n-1}} \frac{\cos \frac{A_{n+1} t_r}{2} - i \frac{b_{n+1}}{A_{n+1}} \sin \frac{A_{n+1} t_r}{2}}{-i \frac{2a_n}{A_n} \sin \frac{A_n t_r}{2}} \quad (30) \end{aligned}$$

should be *almost independent* of n for $n \approx n_{\max}$.

Now observing that for $g'_1 = 0$ we have $a_n = g_1 \sqrt{(2L-n+1)n}$ and $b_n = \omega_1$. Suppose $g_1 \sim \omega_1$ and

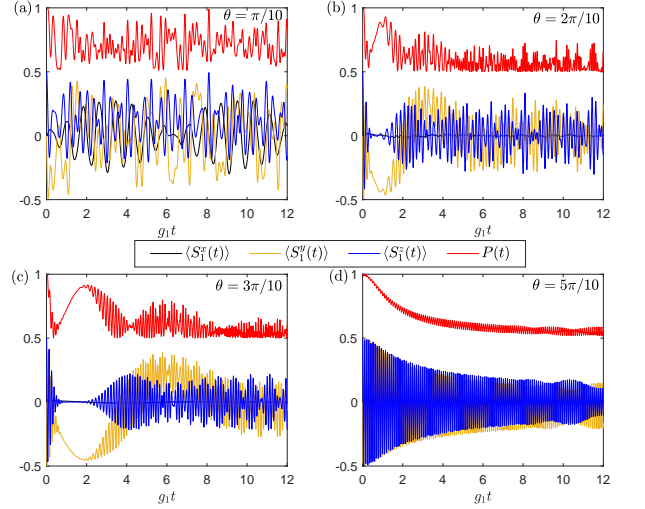


FIG. 2: Time evolution of the three components $\langle S_1^\alpha(t) \rangle$ and the purity $P(t)$ for a single central spin (\vec{S}_1) initially prepared in its up state. Results for $\theta = \pi/10$, $2\pi/10$, $3\pi/10$, and $5\pi/10$ are presented to show the dependence of the dynamics on the bath initial conditions. Parameters: $N = 60$, $\omega_1/g_1 = 1$, $g'_1/g_1 = 0$.

note that $n_{\max} \gg 1$, then $a_n \gg b_n$, so that $A_n \approx 2a_n$. The second term in the numerator of Eq. (30) can thus be neglected, giving

$$\frac{\tilde{F}_\uparrow^{(n)}(t_r)}{\tilde{F}_\downarrow^{(n)}(t_r)} \approx \frac{Q_n}{Q_{n-1}} \frac{\cos \frac{A_{n+1} t_r}{2}}{-i \sin \frac{A_n t_r}{2}} \approx i \frac{\cos \frac{A_{n+1} t_r}{2}}{\sin \frac{A_n t_r}{2}}, \quad (31)$$

where we used the fact that $Q_n \approx Q_{n-1}$ for n around n_{\max} . From Fig. 3(b) we see that A_n decreases with increasing n for $n \geq L$. At the time satisfying

$$t_r = \frac{\pi}{A_n - A_{n+1}}, \quad (32)$$

we have $\cos \frac{A_{n+1} t_r}{2} = \sin \frac{A_n t_r}{2}$, and hence $\tilde{F}_\uparrow^{(n)}(t_r)/\tilde{F}_\downarrow^{(n)}(t_r) \approx i$, which gives an approximately separable state

$$|\psi^{(1)}(t_r)\rangle \approx \frac{1}{\sqrt{2}} (|\uparrow\rangle - i|\downarrow\rangle) \sum_{n \approx n_{\max}} \tilde{F}_\downarrow^{(n)}(t_r) |n-L\rangle. \quad (33)$$

The qubit part of $|\psi^{(1)}(t_r)\rangle$ is just $|-y\rangle$, i.e., the state pointing along the $-y$ direction. For the typical case with $\theta = 3\pi/10$, we have $n_{\max} = 48$ and $(A_{n_{\max}} - A_{n_{\max}+1}) \approx 1.47$, so that $g_1 t_r \approx 2.14$, in consistent with the numerical results presented in Fig. 2(c). For $\theta = \pi/10$ and $5\pi/10$, the frequency difference $A_n - A_{n+1}$ for $n_{\max} = 59$ ($n_{\max} = 30$) is so large (small) [see Fig. 3(b)] that the revival of $P(t)$ occurs at very short (long) time scales [Figs. 2(a),(d)].

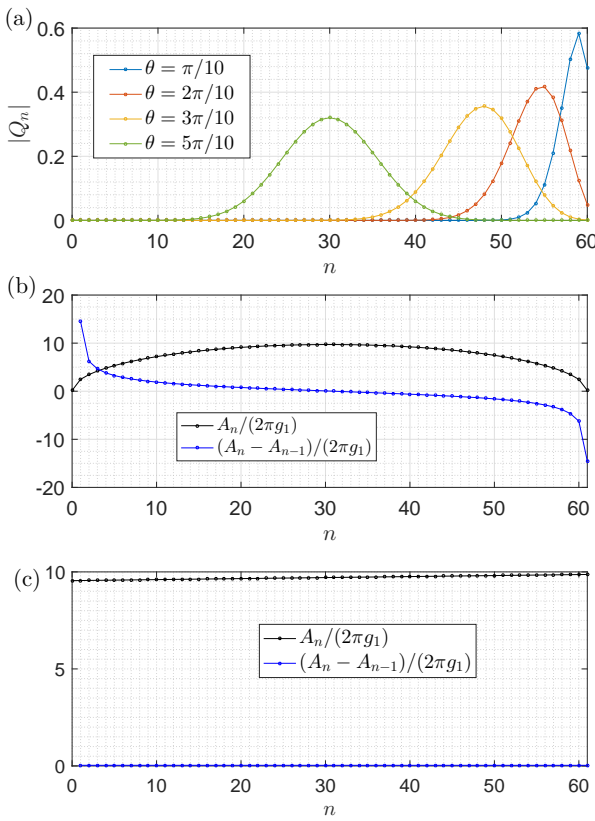


FIG. 3: (a) The dependence of the coefficients $Q_n(\theta, \phi)$ [Eq. (6)] on θ . Note that $|Q_n(\theta, \phi)|^2 = |Q_{N-n}(\pi - \theta, \phi)|^2$. (b) and (c) show the Rabi frequency A_n [Eq. (19)] and the neighboring frequency difference $A_n - A_{n-1}$ for $g'_1 = 0$ and $g'_1 = g_1$, respectively. Parameters: $N = 60$, $\phi = 0$, and $\omega_1/g_1 = 1$.

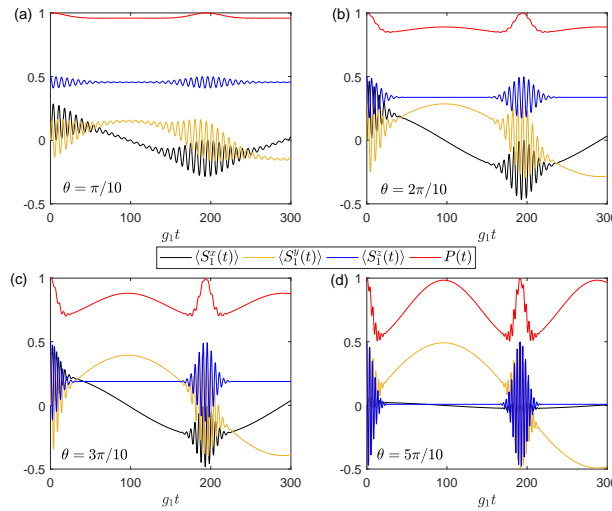


FIG. 4: The same as in Fig. 2, but for $g'_1/g_1 = 1$.

2. XXX -type coupling: $g'_1 = g_1$

In Fig. 4, we plot the dynamics of $\langle S_1^\alpha(t) \rangle$ and $P(t)$ for qubit 1 coupled to the spin bath via XXX -type coupling. We assume $g_1 \approx \omega_1$, then $b_n \approx 2g_1(n - L)$, giving

$$A_n \approx 2g_1\sqrt{L^2 + n} \approx 2g_1L \left(1 + \frac{n}{2L^2}\right). \quad (34)$$

So A_n increases linearly with increasing n with a small slope g_1/L for large L [Fig. 3(c)]. By noting that the frequency difference $A_{n+1} - A_n \approx g_1/L$ is approximately independent of n , revivals of the purity are expected to occur at times satisfying $t_r = (2m + 1)L\pi/g_1$ [Fig. 4(d)].

IV. ENTANGLEMENT AND COHERENCE DYNAMICS OF THE TWO-QUBIT SYSTEM

We now turn to study the reduced dynamics of two qubits homogeneously coupled to spin baths. We will consider two situations, i.e., the two qubits couple to individual baths and to a common bath.

A. Disentanglement of two noninteracting qubits coupled to individual spin baths

The composite system consisting of two qubits interacting with their own environments provides an interesting setup to study the dynamics of entanglement [42, 45, 51]. The single-qubit reduced dynamics obtained in the previous section can be directly used to obtain the reduced dynamics of two such copies, provided that there is *no direct interaction* between the two [45]. The Hamiltonian of such a composite system reads [see Fig. 1(b)]

$$\begin{aligned} H_{\text{ind}} &= \sum_{\alpha=1,2} H_S^{(\alpha)} + H_{SB}^{(\alpha)}, \\ H_S^{(\alpha)} &= \omega_\alpha S_\alpha^z, \\ H_{SB}^{(\alpha)} &= 2 \sum_{j=1}^N \left[g_\alpha (S_\alpha^x T_j^{(\alpha)x} + S_\alpha^y T_j^{(\alpha)y}) + g'_\alpha S_\alpha^z T_j^{(\alpha)z} \right]. \end{aligned} \quad (35)$$

The two baths are independent in the sense that any two operators belonging to distinct copies commute with each other. The entanglement dynamics of a pair of two-level atoms coupled to individual photonic baths is studied in Refs. [42, 45].

Let $\rho(t)$ be the reduced density matrix of the two uncoupled qubits. We assume a separable initial state for the whole system

$$\rho_{\text{tot}}(0) = \rho(0) \otimes \rho_B^{(1)} \otimes \rho_B^{(2)}, \quad (36)$$

where $\rho_B^{(\alpha)}$ is the bath initial state of bath α . For the sake of consistency, we still choose the spin coherent state as

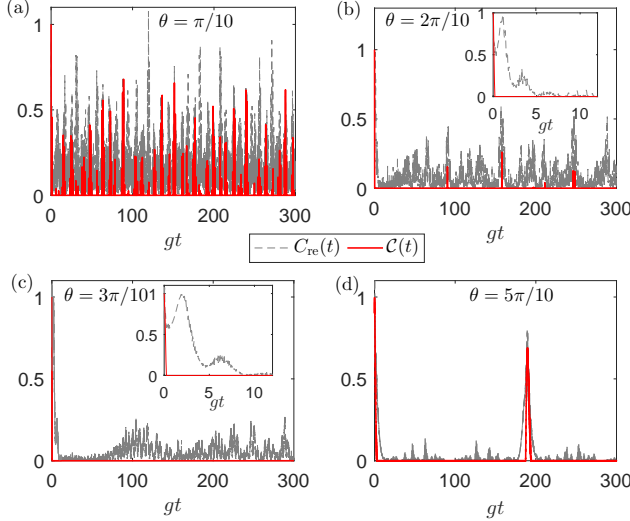


FIG. 5: Time evolution of the relative entropy of coherence $C_{\text{re}}(t)$ (dashed gray curves) and the concurrence $\mathcal{C}(t)$ (red curves) for two qubits independently coupled to their own spin bath via the XX -type coupling [see Eq. (35)]. The initial state of the two qubits is chosen as the maximally entangled state $|\varphi\rangle = \frac{1}{\sqrt{2}}(|\uparrow\downarrow\rangle + |\downarrow\uparrow\rangle)$ and we choose $\theta_1 = \theta_2 = \theta$, $g_1 = g_2 = g$, $\omega_1 = \omega_2 = \omega$, and $g'_1 = g'_2 = g'$ for the two baths. The insets in (b) and (c) shows the corresponding short-time dynamics up to $gt = 12$. Parameters: $N = 60$, $\omega/g = 1$, and $g'/g = 0$.

the bath initial state, i.e., $\rho_B^{(\alpha)} = |\hat{\Omega}^{(\alpha)}\rangle\langle\hat{\Omega}^{(\alpha)}|$. The reduced density matrix $\rho(t)$ can be expressed in the standard basis $\{|\uparrow\uparrow\rangle, |\uparrow\downarrow\rangle, |\downarrow\uparrow\rangle, |\downarrow\downarrow\rangle\}$ as [45]

$$\rho(t)_{aa',bb'} = \sum_{cc'dd'} Y_{abcd}^{(1)}(t) Y_{a'b'c'd'}^{(2)}(t) \rho_{cc',dd'}(0), \quad (37)$$

where $Y_{abcd}^{(1)}(t)$ is determined by the single-qubit dynamics given by Eq. (24).

We focus on the disentanglement dynamics of the maximally entangled state $|\varphi\rangle = (|\uparrow\downarrow\rangle + |\downarrow\uparrow\rangle)/\sqrt{2}$ (so that $\rho(0) = |\varphi\rangle\langle\varphi|$). We use Wootters's concurrence [63] to measure the entanglement between the two qubits, which is defined as

$$\mathcal{C}(t) = \max\{0, \sqrt{\lambda_1} - \sqrt{\lambda_2} - \sqrt{\lambda_3} - \sqrt{\lambda_4}\}, \quad (38)$$

where λ_i are the positive eigenvalues of the matrix $\rho(\sigma_y \otimes \sigma_y) \rho^*(\sigma_y \otimes \sigma_y)$ arranged in decreasing order.

We are also interested in the time evolution of the coherence of the two-qubit state, which is attributed to the off-diagonal elements of the two-qubit reduce density matrix with respect to a selected reference basis. Here, we will use the relative entropy of coherence [64] as a measure of coherence

$$C_{\text{re}}(t) = S(\rho_{\text{diag}}(t)) - S(\rho(t)), \quad (39)$$

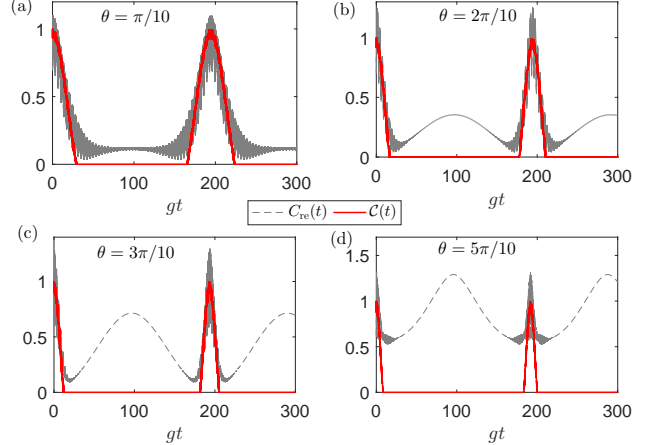


FIG. 6: The same as in Fig. 5, but for the XXX -type coupling with $g'/g = 1$.

where $S(\rho) = -\text{Tr}(\rho \ln \rho)$ is the von Neumann entropy and ρ_{diag} is the density matrix from ρ by removing all off-diagonal elements.

In Fig. 5, we present the time evolution of $C_{\text{re}}(t)$ and $\mathcal{C}(t)$ for the XX -type coupling and various values of θ . Similar to the single-qubit polarization dynamics, both $C_{\text{re}}(t)$ and $\mathcal{C}(t)$ oscillate irregularly for $\theta = \pi/10$. However, for $\theta = 2\pi/10$ we observe an abrupt short decay of the concurrence to zero, which is followed by several revivals peaked at nearly discrete time slices. Similar behaviors are observed for $\theta = 3\pi/10$ and $5\pi/10$. The relative entropy is still present even for vanishing concurrence, indicating that the state of the two qubits might be coherent even in the absence of entanglement between the two. Note that the revival of the concurrence is accompanied by sudden increase in the relative entropy, so the coherence and entanglement are somehow related. Interestingly, we find that the coherence behaves similarly to the single-qubit purity shown in Fig. 3 [by comparing, e.g., Fig. 3(b), (c) with the insets in Fig. 5(b), (c)], indicating the two quantities are positively correlated.

Figure 6 shows the dynamics of $C_{\text{re}}(t)$ and $\mathcal{C}(t)$ for the XXX -type coupling. We see that the two-qubit entanglement decays to zero in a short time for all values of θ considered. After a period of complete disentanglement, a revival of nearly maximal entanglement occurs at $gt \approx N\pi$ (we assume $g_1 = g_2 = g$), a time at which the single-qubit Rabi oscillation also revives (see Fig. 4). Note that similar phenomenon of entanglement disappearance and revival is observed in the non-Markovian dynamics of two noninteracting qubits independently coupled to zero-temperature bosonic reservoirs [45]. Actually, the interaction of quantum spins with a spin bath can in general lead to non-Markovian behavior in the dynamics [58–60]. We also observe a positive correlation between the coherence and the single-qubit purity shown in Fig. 4.

B. Entanglement dynamics of two qubits coupled to a common spin bath

We now consider the reduced two-qubit dynamics governed by Hamiltonian (1), which describes two coupled qubits interacting with a common spin bath via uniform system-bath coupling.

We still assume separable initial state

$$|\psi_0\rangle = |\varphi\rangle|\hat{\Omega}\rangle, \quad (40)$$

where

$$|\varphi\rangle = \sum_{s_1, s_2=\uparrow, \downarrow} A_{s_1, s_2} |s_1, s_2\rangle, \quad (41)$$

with $\sum_{s_1, s_2=\uparrow, \downarrow} |A_{s_1, s_2}|^2 = 1$. There are totally $D_{\text{tot}} = 4(N+1)$ basis states of the form $|s_1, s_2\rangle|n-L\rangle$, and we arrange them as

$$\begin{aligned} & |\downarrow\downarrow\rangle| -L\rangle, \\ & |\uparrow\downarrow\rangle| -L\rangle, |\downarrow\uparrow\rangle| -L\rangle, |\downarrow\downarrow\rangle| -L+1\rangle \\ & |\uparrow\uparrow\rangle| -L\rangle, |\uparrow\downarrow\rangle| -L+1\rangle, |\downarrow\uparrow\rangle| -L+1\rangle, |\downarrow\downarrow\rangle| -L+2\rangle \\ & \vdots \\ & |\uparrow\uparrow\rangle|L-2\rangle, |\uparrow\downarrow\rangle|L-1\rangle, |\downarrow\uparrow\rangle|L-1\rangle, |\downarrow\downarrow\rangle|L\rangle \\ & |\uparrow\uparrow\rangle|L-1\rangle, |\uparrow\downarrow\rangle|L\rangle, |\downarrow\uparrow\rangle|L\rangle, \\ & |\uparrow\uparrow\rangle|L\rangle. \end{aligned} \quad (42)$$

There are $2L+3 = N+3$ rows in the above equation and it is easy to see that $H_I(t)|\downarrow\downarrow\rangle| -L\rangle = H_I(t)|\uparrow\uparrow\rangle|L\rangle = 0$. The time-evolved states in the interaction picture can be expanded in terms these basis states as

$$|\psi_I(t)\rangle = \sum_{s_1, s_2=\uparrow, \downarrow} \sum_{n=0}^N G_{s_1 s_2}^{(n)}(t) |s_1, s_2\rangle |n-L\rangle, \quad (43)$$

with initial conditions $G_{s_1 s_2}^{(n)}(0) = A_{s_1 s_2} Q_n$. Due to the conservation of the magnetization $M = S_1^z + S_2^z + L_z$, the Hamiltonian H is block diagonal in the basis given by Eq. (42), and we can separately treat the time evolution within subspaces spanned by states in each row. As before, application of the Schrödinger equation to the state $|\psi_I(t)\rangle$ leads to the following sets of equations of motion

$$\begin{aligned} i\dot{G}_{\uparrow\uparrow}^{(n-1)} &= G_{\uparrow\uparrow}^{(n)} g_2 x_{n-L-1} e^{i\omega_2 t} e^{-ig'_{12} t} e^{iJ' t} e^{i2g'_2(n-L-1)t} \\ &+ G_{\downarrow\uparrow}^{(n)} g_1 x_{n-L-1} e^{ig'_{12} t} e^{i\omega_1 t} e^{i2g'_1(n-L-1)t} e^{iJ' t}, \\ i\dot{G}_{\uparrow\downarrow}^{(n)} &= G_{\uparrow\downarrow}^{(n)} J e^{i2g'_{12}(n-L)t} e^{i\omega_{12} t} \\ &+ G_{\uparrow\uparrow}^{(n-1)} g_2 x_{n-L-1} e^{ig'_{12} t} e^{-i\omega_2 t} e^{-i2g'_2(n-L-1)t} e^{-iJ' t} \\ &+ G_{\downarrow\downarrow}^{(n+1)} g_1 x_{n-L} e^{-ig'_{12} t} e^{i\omega_1 t} e^{i2g'_1(n-L+1)t} e^{-iJ' t}, \\ i\dot{G}_{\downarrow\uparrow}^{(n)} &= G_{\downarrow\uparrow}^{(n)} J e^{-i2g'_{12}(n-L)t} e^{-i\omega_{12} t} \\ &+ G_{\uparrow\uparrow}^{(n-1)} g_1 x_{n-L-1} e^{-ig'_{12} t} e^{-i\omega_1 t} e^{-i2g'_1(n-L-1)t} e^{-iJ' t} \end{aligned}$$

$$\begin{aligned} &+ G_{\downarrow\downarrow}^{(n+1)} g_2 x_{n-L} e^{-ig'_{12} t} e^{-i\omega_2 t} e^{-i2g'_2(n-L+1)t} e^{iJ' t}, \\ i\dot{G}_{\downarrow\downarrow}^{(n+1)} &= G_{\downarrow\downarrow}^{(n)} g_1 x_{n-L} e^{-i\omega_1 t} e^{ig'_{12} t} e^{iJ' t} e^{-i2g'_1(n-L+1)t} \\ &+ G_{\uparrow\downarrow}^{(n)} g_2 x_{n-L} e^{-ig'_{12} t} e^{-i\omega_2 t} e^{-i2g'_2(n-L+1)t} e^{iJ' t}, \end{aligned} \quad (44)$$

for $n = 1, 2, \dots, N-1$. The above set of equations can also incorporate the cases with $n=0$ and $n=N+1$, with the understanding that $G_{s_1 s_2}^{(-1)} = G_{s_1 s_2}^{(N+1)} \equiv 0$. In contrast to the single-qubit dynamics, these coupled equations of motion can no longer be solved analytically.

The Schrödinger picture wave function is

$$\begin{aligned} |\psi(t)\rangle &= e^{-iH_0 t} |\psi_I(t)\rangle \\ &\equiv \sum_{s_1, s_2=\uparrow, \downarrow} \sum_{n=0}^N \tilde{G}_{s_1 s_2}^{(n)}(t) |s_1, s_2\rangle |n-L\rangle, \end{aligned} \quad (45)$$

where

$$\begin{aligned} \tilde{G}_{s_1 s_2}^{(n)}(t) &= G_{s_1 s_2}^{(n)}(t) e^{-\frac{i}{2}(v_1\omega_1 + v_2\omega_2 + J' v_1 v_2)t} \\ &\quad e^{-i(g'_1 v_1 + g'_2 v_2)(n-L)t}, \end{aligned} \quad (46)$$

with $v_i = 1$ or -1 for $s_i = \uparrow$ or \downarrow .

The reduced density matrix (in the standard basis) of the two qubits can be obtained by tracing out the bath degrees of freedom

$$\begin{aligned} \rho(t) &= \text{Tr}_B[|\psi(t)\rangle\langle\psi(t)|] \\ &= \sum_{s_1, s_2} \sum_{s'_1, s'_2} \sum_{n=0}^N \tilde{G}_{s_1 s_2}^{(n)}(t) \tilde{G}_{s'_1 s'_2}^{(n)*}(t) |s_1 s_2\rangle\langle s'_1 s'_2| \\ &= \begin{pmatrix} C_{\uparrow\uparrow; \uparrow\uparrow} & C_{\uparrow\uparrow; \uparrow\downarrow} & C_{\uparrow\uparrow; \downarrow\uparrow} & C_{\uparrow\uparrow; \downarrow\downarrow} \\ C_{\uparrow\downarrow; \uparrow\uparrow} & C_{\uparrow\downarrow; \uparrow\downarrow} & C_{\uparrow\downarrow; \downarrow\uparrow} & C_{\uparrow\downarrow; \downarrow\downarrow} \\ C_{\downarrow\uparrow; \uparrow\uparrow} & C_{\downarrow\uparrow; \uparrow\downarrow} & C_{\downarrow\uparrow; \downarrow\uparrow} & C_{\downarrow\uparrow; \downarrow\downarrow} \\ C_{\downarrow\downarrow; \uparrow\uparrow} & C_{\downarrow\downarrow; \uparrow\downarrow} & C_{\downarrow\downarrow; \downarrow\uparrow} & C_{\downarrow\downarrow; \downarrow\downarrow} \end{pmatrix}, \end{aligned} \quad (47)$$

where

$$C_{s_1 s_2; s'_1 s'_2}(t) = \sum_{n=0}^N \tilde{G}_{s_1 s_2}^{(n)}(t) \tilde{G}_{s'_1 s'_2}^{(n)*}(t). \quad (48)$$

In this subsection, we will focus on the case of XXX -type coupling. In Fig. 7 we show the disentanglement dynamics of the two qubits starting with the maximally entangled state $|\varphi\rangle = (|\uparrow\downarrow\rangle + |\downarrow\uparrow\rangle)/\sqrt{2}$. Unlike the case of individual baths for which the profiles of the disentanglement dynamics behave similarly for different θ 's, here the entanglement dynamics depends sensitively on θ . For $\theta = \pi/10$, the bath initial state $|\hat{\Omega}\rangle$ is close to the fully polarized state $|L\rangle$ so that the time evolution mainly takes place in the subspace spanned by the basis states in the last few lines of Eq. (42), which results in a oscillatory behavior between 1 and 0.5. For $\theta = 2\pi/10$, we observe collapse and revival behaviors for both the concurrence and the coherence with period $\approx L\pi$. As θ is increased further, sudden disappearance and revival of the concurrence occurs. We note that collapse and

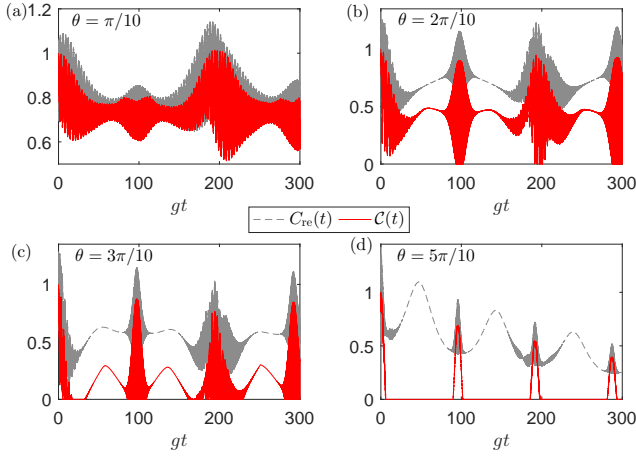


FIG. 7: Time evolution of the relative entropy of coherence $C_{\text{re}}(t)$ (dashed gray curves) and the concurrence $C(t)$ (red curves) for two qubits coupled to a common spin bath via the XXX -type coupling. The initial state is chosen as the maximally entangled state $|\varphi\rangle = \frac{1}{\sqrt{2}}(|\uparrow\downarrow\rangle + |\downarrow\uparrow\rangle)$ and we choose $g_1 = g_2 = g$, $\omega_1 = \omega_2 = \omega$, and $g'_1 = g'_2 = g'$. Parameters: $N = 60$, $\omega/g = 1$, $g'/g = 1$, and $J/g = J'/g = 0$.

revival behaviors in the entanglement dynamics of two qubits coupled to a single bosonic mode was revealed in Ref. [66].

In the case of individual baths, two initially unentangled noninteracting qubits can never get entangled. In contrast, it is well known that two noninteracting qubits coupled to a common spin bath can become entangled even starting with an unentangled state. Figure 8 shows the entanglement generation of two initially separable qubits prepared in the state $|\psi(0)\rangle = |\uparrow\uparrow\rangle$. We again observe the collapse and revival phenomena in the dynamics of both $C_{\text{re}}(t)$ and $C(t)$ for large values of θ . Moreover, $C(t)$ can keep a finite steady value for a relatively long time period of time in the duration of the collapse [Fig. 8(c) and (d)]. This provides a possible scenario to create steady entanglement between the two qubits via their couplings to the common spin bath.

V. CONCLUSIONS

In this work, we obtain benchmark exact quantum dynamics of the two-qubit homogeneous central spin model with the spin bath prepared in the spin coherent state. By working in the interaction picture with respect to the non-spin-flipping part of the Hamiltonian, we derive a set of equations of motion satisfied by the amplitudes of the time-evolved wave function. For a single-qubit central spin problem, the equations of motion can be an-

alytically solved to give closed-form expressions for the amplitudes, recovering the results in Ref. [37]. These analytical results are then used to study the time-evolution

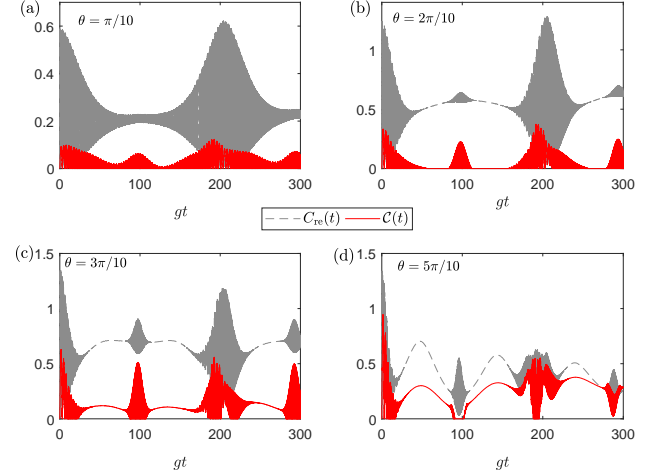


FIG. 8: The same as in Fig. 7, but for a separable two-qubit initial state $|\varphi\rangle = |\uparrow\uparrow\rangle$.

of the single-qubit polarization and purity dynamics. The observed collapse and revival phenomena are explained in a quantitative way following an analogical analysis in Ref. [62] on the Jaynes-Cummings model.

We then study the disentanglement dynamics of two initially entangled noninteracting qubits interacting with individual baths. The dynamics of such a system can be directly determined by the single-qubit dynamics following the procedures presented in Ref. [45]. We calculate the time-evolution of the concurrence and relative entropy of coherence of the two-qubit system. We find that the two-qubit coherence behaves similarly to the single-qubit purity. Due to the non-Markovian nature of the spin bath, we observe entanglement sudden disappearance in a finite time, and the subsequent revivals. We finally study the entanglement generation process between the two initially unentangled qubits caused by the coupling to a common spin bath. For certain bath initial states, we observe collapse and revival behaviors in the entanglement and coherence dynamics, which provides a possible setup to realize steady and finite two-qubit entanglement or coherence over long periods of time.

Acknowledgments: This work was supported by the Natural Science Foundation of China (NSFC) under Grant No. 11705007, and partially by the Beijing Institute of Technology Research Fund Program for Young Scholars. W.-L. Y. acknowledge support from the start-up fund of Nanjing University of Aeronautics and Astronautics (Grant No. 1008-YAH20006).

[1] N. V. Prokofev and P. C. E. Stamp, *Rep. Prog. Phys.* **63**, 669 (2000).

[2] F. M. Cucchietti, J. P. Paz, and W. H. Zurek, *Phys. Rev. A* **72**, 052113 (2005).

[3] C. M. Dawson, A. P. Hines, R. H. McKenzie, and G. J. Milburn, *Phys. Rev. A* **71**, 052321 (2005).

[4] H. T. Quan, Z. Song, X. F. Liu, P. Zanardi, and C. P. Sun, *Phys. Rev. Lett.* **96**, 140604 (2006).

[5] Y. Hamdouni and F. Petruccione, *Phys. Rev. B* **76**, 174306 (2007).

[6] S. Takahashi, R. Hanson, J. van Tol, M. S. Sherwin, and D. D. Awschalom, *Phys. Rev. Lett.* **101**, 047601 (2008).

[7] W. M. Witzel and S. Das Sarma, *Phys. Rev. B* **77**, 165319 (2008).

[8] C. Y. Lai, J. T. Hung, C. Y. Mou, and P. Chen, *Phys. Rev. B* **77**, 205419 (2008).

[9] N. Zhao, Z.-Y. Wang, and R.-B. Liu, *Phys. Rev. Lett.* **106**, 217205 (2011).

[10] A. Faribault and D. Schuricht, *Phys. Rev. B* **88**, 085323 (2013).

[11] Z.-H. Wang and S. Takahashi, *Phys. Rev. B* **87**, 115122 (2013).

[12] S. Dooley, F. McCrossan, D. Harland, M. J. Everitt, and T. P. Spiller, *Phys. Rev. A* **87**, 052323 (2013).

[13] N. Wu, A. Nanduri, and H. Rabitz, *Phys. Rev. A* **89**, 062105 (2014).

[14] N. Wu, N. Fröhling, X. Xing, J. Hackmann, A. Nanduri, F.B. Anders, and H. Rabitz, *Phys. Rev. B* **93**, 035430 (2016).

[15] D. Kwiatkowski and L. Cywiński, *Phys. Rev. B* **98**, 155202 (2018).

[16] P. Lu, H.-L. Shi, L. Cao, X.-H. Wang, T. Yang, J. Cao, and W.-L. Yang, *Phys. Rev. B* **101**, 184307 (2020).

[17] A. V. Khaetskii, D. Loss, and L. Glazman, *Phys. Rev. Lett.* **88**, 186802 (2002).

[18] A. V. Khaetskii, D. Loss, and L. Glazman, *Phys. Rev. B* **67**, 195329 (2003).

[19] A. Hutton and S. Bose, *Phys. Rev. A* **69**, 042312 (2004).

[20] X. Z. Yuan, H. S. Goan, and K. D. Zhu, *Phys. Rev. B* **75**, 045331 (2007).

[21] H. Christ, J. I. Cirac, and G. Giedke, *Phys. Rev. B* **78**, 125314 (2008).

[22] G.-Q. Liu, *et al.*, *Phys. Rev. Lett.* **118**, 150504 (2017).

[23] F. Wang, *et al.*, *Phys. Rev. B* **98**, 064306 (2018).

[24] L. Dong, H. Liang, C.-K. Duan, Y. Wang, Z. Li, X. Rong, J. Du, *Phys. Rev. A* **99**, 013426 (2019).

[25] A. Olaya-Castro, C. F. Lee, F. F. Olsen, and N. F. Johnson, *Phys. Rev. B* **78**, 085115 (2008).

[26] I. Sinayskiy, A. Marais, F. Petruccione, and A. Ekert, *Phys. Rev. Lett.* **108**, 020602 (2012).

[27] N. Wu and Y. Zhao, *J. Chem. Phys.* **139**, 054118 (2013).

[28] M. Gaudin, *J. Phys. France* **37**, 1087 (1976).

[29] D. Garajeu and A. Kiss, *J. Math. Phys.* **42**, 3497 (2001).

[30] G. Ortiz, R. Somma, J. Dukelsky, and S. Rombouts, *Nucl. Phys. B* **707**, 421 (2005).

[31] M. Bortz and J. Stolze, *Phys. Rev. B* **76**, 014304 (2007).

[32] B. Erbe and J. Schliemann, *Phys. Rev. Lett.* **105**, 177602 (2010).

[33] P. W. Claeys, S. De Baerdemacker, M. Van Raemdonck, and D. Van Neck, *Phys. Rev. B* **91**, 155102 (2015).

[34] N. Wu, *Physica A* **501**, 308 (2018).

[35] R. I. Nepomechie and X.-W. Guan, *J. Stat. Mech.* (2018) 103104.

[36] T. Skrypnyk, *Nucl. Phys. B* **941**, 225 (2019).

[37] W.-B. He, S. Chesi, H.-Q. Lin, and X.-W. Guan, *Phys. Rev. B* **99**, 174308 (2019).

[38] N. Wu, X.-W. Guan, and J. Links, *Phys. Rev. B* **101**, 155145 (2020).

[39] T. Villazon, A. Chandran, and P. W. Claeys, arXiv:2001.10008.

[40] D. Braun, *Phys. Rev. Lett.* **89**, 277901 (2002).

[41] F. Benatti, R. Floreanini, and M. Piani, *Phys. Rev. Lett.* **91**, 070402 (2003).

[42] T. Yu and J. H. Eberly, *Phys. Rev. Lett.* **93**, 140404 (2004).

[43] S. Oh and J. Kim, *Phys. Rev. A* **73**, 062306 (2006).

[44] M. P. Almeida, F. de Melo, M. Hor-Meyll, A. Salles, S. P. Walborn, P. H. Souto Ribeiro, L. Davidovich, *Science* **316**, 579 (2007).

[45] B. Bellomo, R. Lo Franco, and G. Compagno, *Phys. Rev. Lett.* **99**, 160502 (2007).

[46] D. Solenov, D. Tolkunov, and V. Privman, *Phys. Rev. B* **75**, 035134 (2007).

[47] J. Dajka, M. Mierzejewski, and J. Luczka, *Phys. Rev. A* **77**, 042316 (2008).

[48] S. Maniscalco, F. Francica, R. L. Zaffino, N. Lo Gullo, and F. Plastina, *Phys. Rev. Lett.* **100**, 090503 (2008).

[49] L. D. Contreras-Pulido and R. Aguado, *Phys. Rev. B* **77**, 155420 (2008).

[50] D. P. S. McCutcheon, A. Nazir, S. Bose, and A. J. Fisher, *Phys. Rev. A* **80**, 022337 (2009).

[51] A. G. Dijkstra and Y. Tanimura, *Phys. Rev. Lett.* **104**, 250401 (2010).

[52] X. Zhao, J. Jing, B. Corn, and T. Yu, *Phys. Rev. A* **84**, 032101 (2011).

[53] J. Ma, Z. Sun, X. Wang, and F. Nori, *Phys. Rev. A* **85**, 062323 (2012).

[54] N. Qiu and X.-B. Wang, *Phys. Rev. A* **88**, 062332 (2013).

[55] M. M. Sahrapour and N. Makri, *J. Chem. Phys.* **138**, 114109 (2013).

[56] D. Kast and J. Ankerhold, *Phys. Rev. B* **90**, 100301(R) (2014).

[57] J. She, J. Hu, and H. Yu, *Phys. Rev. D* **99**, 105009 (2019).

[58] H. Krovi, O. Oreshkov, M. Ryazanov, and D. A. Lidar, *Phys. Rev. A* **76**, 052117 (2007).

[59] E. Ferraro, H.-P. Breuer, A. Napoli, M. A. Jivulescu, and A. Messina, *Phys. Rev. B* **78**, 064309 (2008).

[60] S. Lorenzo, F. Plastina, and M. Paternostro, *Phys. Rev. A* **87**, 022317 (2013).

[61] M. Lucamarini, S. Paganelli, and S. Mancini, *Phys. Rev. A* **69**, 062308 (2004).

[62] J. Gea-Banacloche, *Phys. Rev. Lett.* **65**, 3385 (1990).

[63] W. K. Wootters, *Phys. Rev. Lett.* **80**, 2245 (1998).

[64] T. Baumgratz, M. Cramer, and M.B. Plenio, *Phys. Rev. Lett.* **113**, 140401 (2014).

[65] F. T. Arecchi, E. Courtens, R. Gilmore, and H. Thomas, *Phys. Rev. A* **6**, 2211 (1972).

[66] V. S. Malinovsky and I. R. Sola, *Phys. Rev. Lett.* **96**, 050502 (2006).

Appendix A: On the spin coherent state

The spin coherent state of the N spins-1/2 is defined as

$$\begin{aligned} |\hat{\Omega}\rangle &= e^{-iL_z\phi}e^{-iL_y\theta}\left|\frac{N}{2}, \frac{N}{2}\right\rangle \\ &= \prod_{j=1}^N e^{-iT_j^z\phi}e^{-iT_j^y\theta}|+\rangle_j \\ &= \prod_{j=1}^N \left[\cos \frac{\theta}{2} e^{-i\phi/2}|+\rangle_j + \sin \frac{\theta}{2} e^{i\phi/2}|-\rangle_j \right], \end{aligned} \quad (\text{A1})$$

where $|+\rangle_j$ is the spin-up state for the j th bath spin. By expanding the right-hand side of Eq. (A1), $|\hat{\Omega}\rangle$ can be rewritten as

$$\begin{aligned} |\hat{\Omega}\rangle &= \sum_{m=0}^N \left(\cos \frac{\theta}{2} \right)^m \left(\sin \frac{\theta}{2} \right)^{N-m} e^{i\phi(N-2m)/2} \\ &\quad \sum_{n_1 < n_2 < \dots < n_{N-m}} T_{n_1}^- \cdots T_{n_{N-m}}^- \left(\prod_{j=1}^N |+\rangle_j \right). \end{aligned} \quad (\text{A2})$$

Recall that the Dicke states can be expressed as

$$\begin{aligned} &\left|\frac{N}{2}, m - \frac{N}{2}\right\rangle \\ &= \frac{1}{\sqrt{C_N^m}} \sum_{n_1 < n_2 < \dots < n_{N-m}} T_{n_1}^- \cdots T_{n_{N-m}}^- \left(\prod_{j=1}^N |+\rangle_j \right), \end{aligned} \quad (\text{A3})$$

we thus have

$$\begin{aligned} |\hat{\Omega}\rangle &= \sum_{m=0}^N \left(\cos \frac{\theta}{2} \right)^m \left(\sin \frac{\theta}{2} \right)^{N-m} \\ &\quad e^{i\phi(N-2m)/2} \sqrt{C_N^m} \left| \frac{N}{2}, m - \frac{N}{2} \right\rangle. \end{aligned} \quad (\text{A4})$$

Up to a global phase factor $e^{i\phi N/2}$, the spin coherent state $|\hat{\Omega}\rangle$ can finally be written as

$$|\hat{\Omega}\rangle = \sum_{n=0}^N Q_n \left| \frac{N}{2}, n - \frac{N}{2} \right\rangle, \quad (\text{A5})$$

where

$$Q_n \equiv \frac{z^n}{(1+|z|^2)^{N/2}} \sqrt{C_N^m}, \quad (\text{A6})$$

with $z = \cot \frac{\theta}{2} e^{-i\phi}$.

Appendix B: Equations of motion for a single-qubit in the $M = m - \frac{1}{2}$ sector

Consider a typical evolved state governed by $H_I^{(1)}(t)$ in the $M = m - \frac{1}{2}$ sector (let $|m\rangle = |\frac{N}{2}, m\rangle$),

$$|\chi^{(m)}(t)\rangle = C_{\uparrow}^{(m)}(t)|\uparrow\rangle|m-1\rangle + C_{\downarrow}^{(m)}(t)|\downarrow\rangle|m\rangle. \quad (\text{B1})$$

Applying the Schrödinger operator $H_I^{(1)}(t)$ to the above state, we get

$$\begin{aligned} &H_I^{(1)}(t)|\chi^{(m)}(t)\rangle \\ &= C_{\uparrow}^{(m)}(t)g_1 e^{-i\omega_1 t} e^{-i2g_1' m t} e^{ig_1' t} x_{l,m-1} |\downarrow\rangle|m\rangle \\ &\quad + C_{\downarrow}^{(m)}(t)g_1 x_{l,m-1} e^{-ig_1' t} e^{i2g_1' m t} e^{i\omega_1 t} |\uparrow\rangle|m-1\rangle. \end{aligned} \quad (\text{B2})$$

From the Schrödinger equation $i\partial_t|\chi^{(m)}(t)\rangle = H_I^{(1)}(t)|\chi^{(m)}(t)\rangle$, we obtain the following equations of motion for the coefficients $C_{\uparrow/\downarrow}^{(m)}(t)$

$$\begin{aligned} i\dot{C}_{\uparrow}^{(m)}(t) &= C_{-}^{(m)}(t)g_1 x_{l,m-1}^{(-)} e^{-ig_1' t} e^{i2g_1' m t} e^{i\omega_1 t}, \\ i\dot{C}_{\downarrow}^{(m)}(t) &= C_{+}^{(m)}(t)g_1 x_{l,m-1}^{(-)} e^{-i\omega_1 t} e^{-i2g_1' m t} e^{ig_1' t}. \end{aligned} \quad (\text{B3})$$

Appendix C: Analytical solutions of Eq. (14)

We provide the analytical solution to the following two coupled first-order ordinary differential equations

$$\begin{aligned} i\dot{x}_1 &= ae^{ibt}x_2, \\ i\dot{x}_2 &= ae^{-ibt}x_1, \end{aligned} \quad (\text{C1})$$

under the initial condition

$$x_1(0) = X_1, \quad x_2(0) = X_2, \quad (\text{C2})$$

where a and b are two real constants.

We first differentiate the first equation once to get

$$\ddot{x}_1 - ib\dot{x}_1 + a^2 x_1 = 0. \quad (\text{C3})$$

The characteristic equation for the last equation is

$$\lambda^2 - ib\lambda + a^2 = 0, \quad (\text{C4})$$

which gives two distinct imaginary roots

$$\lambda_{\pm} = \frac{i}{2}(b \pm \sqrt{b^2 + 4a^2}) \quad (\text{C5})$$

So the general solution is

$$x_1 = c_+ e^{\lambda_+ t} + c_- e^{\lambda_- t} \quad (\text{C6})$$

with

$$c_+ + c_- = X_1. \quad (\text{C7})$$

The other variable $x_2(t)$ can be obtained as

$$\begin{aligned} x_2 &= \frac{i}{a} e^{-ibt} \dot{x}_1 \\ &= \frac{i}{a} e^{-ibt} (c_+ \lambda_+ e^{\lambda_+ t} + c_- \lambda_- e^{\lambda_- t}) \end{aligned} \quad (\text{C8})$$

so that

$$X_2 = \frac{i}{a} (c_+ \lambda_+ + c_- \lambda_-) \quad (\text{C9})$$

Solving Eqs. (C7) and (C9) gives

$$\begin{aligned} c_- &= -i \frac{\lambda_+}{A} X_1 + \frac{a}{A} X_2, \\ c_+ &= \frac{i \lambda_-}{A} X_1 - \frac{a}{A} X_2, \end{aligned} \quad (\text{C10})$$

where $A \equiv \sqrt{b^2 + 4a^2}$. By inserting the coefficients c_{\pm} into Eqs. (C6) and (C8), we finally get the solution

$$\begin{aligned} x_1 &= e^{\frac{i}{2}bt} \left[X_1 \cos \frac{At}{2} - i \left(\frac{b}{A} X_1 + \frac{2a}{A} X_2 \right) \sin \frac{At}{2} \right], \\ x_2 &= e^{-\frac{i}{2}bt} \left[X_2 \cos \frac{At}{2} + i \left(\frac{-2a}{A} X_1 + \frac{b}{A} X_2 \right) \sin \frac{At}{2} \right]. \end{aligned} \quad (\text{C11})$$

Appendix D: Explicit forms of the coefficients $\{Y_{abcd}(t)\}$ in Eq. (24)

Direct calculations based on Eqs. (16) and (21) give the following explicit forms of $Y_{abcd}(t)$:

$$Y_{\uparrow\uparrow\uparrow\uparrow} = \sum_{n=0}^N |Q_n|^2 |W_{n+1}|^2, \quad Y_{\uparrow\uparrow\downarrow\downarrow} = \sum_{n=1}^N |Q_n|^2 |V_n|^2,$$

$$Y_{\uparrow\uparrow\uparrow\downarrow} = Y_{\uparrow\uparrow\downarrow\uparrow}^* = \sum_{n=1}^N Q_{n-1} Q_n^* W_n V_n^*, \quad (\text{D1})$$

$$\begin{aligned} Y_{\downarrow\downarrow\uparrow\uparrow} &= \sum_{n=1}^N |Q_{n-1}|^2 |V_n|^2, \quad Y_{\downarrow\downarrow\downarrow\downarrow} = \sum_{n=0}^N |Q_n|^2 |W_n|^2, \\ Y_{\downarrow\downarrow\uparrow\downarrow} &= Y_{\downarrow\downarrow\downarrow\uparrow}^* = \sum_{n=1}^N Q_{n-1} Q_n^* W_n V_n, \end{aligned} \quad (\text{D2})$$

and

$$\begin{aligned} Y_{\uparrow\uparrow\uparrow\uparrow} &= Y_{\downarrow\uparrow\uparrow\uparrow}^* = \sum_{n=1}^N Q_n Q_{n-1}^* W_{n+1} V_n^*, \\ Y_{\uparrow\uparrow\downarrow\downarrow} &= Y_{\downarrow\uparrow\downarrow\downarrow}^* = \sum_{n=1}^N Q_{n-1}^* Q_n W_{n-1} V_n, \\ Y_{\uparrow\downarrow\uparrow\downarrow} &= Y_{\downarrow\uparrow\downarrow\uparrow}^* = \sum_{n=0}^N |Q_n|^2 W_n W_{n+1}, \\ Y_{\uparrow\downarrow\downarrow\uparrow} &= Y_{\downarrow\uparrow\uparrow\downarrow}^* = \sum_{n=1}^{N-1} Q_{n-1}^* Q_{n+1} V_n^* V_{n+1}. \end{aligned} \quad (\text{D3})$$